*Journal of Photoscience* (2005), Vol. 12(1), pp. 17-23

# $TiO_2$-Encapsulated EFAL-Removed Zeolite Y as a New Photocatalyst for Photodegradation of Azo Dyes in Aqueous Solution

Won-Je Cho, Sook-Ja Yoon and Minjoong Yoon*
Molecular/Nano Photochemistry & Photonics Laboratory, Department of Chemistry
Chungnam National University Daejeon 305-764, Korea

Application of a new photocatalyst has been attempted to improve the efficiency and rates of photocatalytic degradation of azo dyes by using a model dye such as Methyl Orange (MO). As a new photocatalyst, $TiO_2$-encapsulated EFAL-removed zeolite Y ($TiO_2$/EFAL-removed zeolite Y) has been synthesized by ion-exchange in the mixture of EFAL-removed zeolite Y with 0.05 M aqueous $[(NH_4)_2\ TiO(C_2O_4)_2.H_2O]$. This new photocatalyst has been characterized by measuring XRD, IR and reflectance absorption spectra as well as ICP analysis, and it was found that the framework structure of $TiO_2$/EFAL-removed zeolite Y is not changed by removing the extra-framework aluminum (EFAL) from the normal zeolite Y and the $TiO_2$ inside the photocatalyst exists in the form of $(TiO^{2+})_n$ nanoclusters. Based on the ICP analysis, the Si/Al ratio of the $TiO_2$/EFAL-removed zeolite Y and the weight of $TiO_2$ were determined to be 23 and 0.061 g in 1.0 g photocatalyst, respectively. It was also found that adsorption of the azo dye in the $TiO_2$/EFAL-removed zeolite is very effective (about 80 % of the substrate used). This efficient adsorption contributes to the synergistic photocatalytic activities of the $TiO_2$/EFAL-removed zeolite by minimizing the required flux diffusion of the substrate. Thus, the photocatalytic reduction of MO was found to be 8 times more effective in the presence of $TiO_2$ /EFAL-removed zeolite Y than in the presence of $TiO_2$ /normal zeolite Y. Furthermore, the photocatalytic reduction of MO by using 1.0 g of the $TiO_2$ /EFAL-removed zeolite Y containing 0.061g of $TiO_2$ is much faster than that carried out by using 1.0 g of Degussa P-25.

**key words:** Photocatalyst, $TiO_2$, EFAL-removed zeolite Y, Zeolite Y, Degussa P-25, Methyl Orange, Azo Dyes, Photodegradation, Photoreduction

## INTRODUCTION

A large number of organic dyestuffs (about 10,000 species) have been used in the textile industry [1]. Over 50% of those dyes consist of azo dyes, and they generate very toxic and mutagenic wastewater in dyeing process of textiles [2-4]. These hazardous effluents have been removed for the environmental cleaning of water by using physicochemical, oxidative, or most commonly, active sludge biochemical processes. However, these processes have main drawback such as production of secondary pollutants due to the possible accumulations of other chemicals and bio-resistant species in the water environment. Moreover, the homogeneous and aerobic oxidation treatments are usually effective towards the decoloration by destruction of chromophoric structures of azo dyes, but the mineralization is not often completed. Also, solubility of azo dyes in water is not so high, and only few azo dyes can be successfully oxidized aerobically. In order to overcome these problems, several methods of heterogeneous photocatalysis have been employed for the photodegradation of several azo dyes on a bench scale with artificial [5-9] and solar [10-12] irradiation.

Several semiconductors are useful for the photocatalysis of water pollutants because they can catalyze both photo-oxidation and photo-reduction of the organic substrates through the photo-induced generation of electrons and holes. Among those semiconductors, $TiO_2$ is known to be the most commonly used and effective because it is inexpensive, photo-stable, chemically and biologically inert without induction of the second pollution of water. Several crystalline types of $TiO_2$ photocatalyst have been used, but particularly polycrystalline nanoporous $TiO_2$ powder (Degussa P25, ca. 80% anatase and 20% rutile, BET surface area ca. 50 $m^2\ g^{-1}$) was mostly used for the effective destruction of dyes in waste water [13]. Nevertheless, these powders cannot be recycled due to the small particle sizes. Moreover, the crystalline $TiO_2$ powders have the strong polar surface enough to prevent adsorption of neutral organic substrates. In order to avoid these problems, ceramics [14], fiber glass and active carbons [15] have been used as $TiO_2$ supporters, but these supporters cut down the absorption of light so that the photocatalytic efficiency is limited. Thus, nanoporous zeolites have been introduced to support $TiO_2$ inside of their supercages. It has been believed that the frame of the zeolite supercage limits the recombination of electron-hole photo-generated from $TiO_2$, enhancing the photocatalytic activity of $TiO_2$. However,

* To whom correspondence should be addressed.
E-mail : myoon@cnu.ac.kr
Received & Accepted;

the supercages of normal zeolite have polar environments due to the frame structure consisted of aluminum oxides $[AlO_4]_y$ and silicon oxides $[SiO_4]_x$, and it still limits the adsorption of organic substrates so that the normal zeolite system does not cause remarkable improvement of the photocatalytic efficiency of $TiO_2$.

Recently, in order to increase the photocatalytic activity, modification of the normal zeolite frame has been attempted by controlling the Si/Al ratio through removing an extra-framework-aluminum (EFAL) [16-18]. The removal of EFAL is known to improve the surface characteristics of the normal zeolite [19], and the EFAL-removed zeolite has been expected to be effectively used as a catalyst by increasing the adsorption.of the substrate. Nevertheless, it has not been practically used as a general catalyst, moreover as a photocatalyst by combining it with $TiO_2$. Therefore, in this work, the $TiO_2$ nanoclusters-encapsulated EFAL-removed zeolite Y ($TiO_2$/EFAL-removed zeolite Y) was synthesized and characterized as a new photocatalyst. In order to confirm the photocatalytic activity to decompose an azo dye in water, the photocatalytic reduction of Methyl Orange (MO) was carried out in aqueous suspension of the $TiO_2$/EFAL-removed zeolite Y and compared with the results obtained with $TiO_2$-encapsulated normal zeolite Y ($TiO_2$/normal zeolite Y) or Degussa P25.

## EXPERIMENTAL SECTION

*Materials*

NaY zeolites, ammonium titanyl oxalate mono-hydrate $[(NH_4)_2 TiO(C_2O_4)_2.H_2O]$, methyl orange (MO) and all the other chemical reagents were purchased from Aldrich Co. and used without any further purification. Degussa P25 was purchased from Degussa-Huls.

*Synthesis of $TiO_2$/normal zeolite Y and $TiO_2$/EFAL-removed zeolite Y*

$TiO_2$/normal zeolite Y was synthesized by ion exchange HY zeolite with 0.05 M aqueous $[(NH_4)_2TiO(C_2O_4)_2.H_2O]$ [20]. The HY zeolite was prepared by ion exchange of 0.1 M $NH_4Cl$ solution with 5g NaY zeolite as described in the reference [21]. The ion-exchanged HY zeolite with $TiO_2$ ($TiO_2$-entrapped normal zeolite Y) was found to contain 7.2 Ti per unit cell. This $TiO_2$/normal zeolite Y was washed three times with triply distilled water in order to remove unnecessary adsorbed materials, followed by drying in oven. The dried zeolites were calcinated at 450°C for 12 hrs.

$TiO_2$/EFAL-removed zeolite Y was prepared by ion exchange of EFAL-removed zeolite Y with 0.05 M aqueous $[(NH_4)_2TiO(C_2O_4)_2.H_2O]$. The EFAL-removed zeolite Y was synthesized by steaming method as described in the reference [19]. According to this method, HY zeolite was steamed at 650°C for 4 hrs and dried at 400°C for 2 hrs. Thereafter, the steamed HY zeolite was treated with 2N nitric acid (5 ml/g zeolite) and heated at 100°C for 2 hrs. The acid-treated zeolite was washed with triply distilled water, followed by calcinations at 550°C for 5 more hrs.

*Photocatalysis and Photolysis*

Photocatalysis and photolysis experiments were performed in the pyrex vessel by using irradiation lamp as shown in Figure 1. The irradiation lamp, Hanovia medium pressure Xe arc lamp (150 W), was set inside the air-circulating house so that it can be cooled during irradiation. The lamp housing was placed next to the reaction vessel attached to a cut-off filter to remove the light with wavelength shorter than 280 nm. The distance between the sample vessel and the lamp was adjusted so that the incident power of lamp was 0.5 W. This set-up prohibits the photolysis of MO by itself without the catalyst. Actually MO can be decomposed by both photoreduction and photooxidation. In order to avoid the confusion of the photocatalysis mechanism, the photocatalysis and photolysis experiments were performed under the photoreduction condition. Thus, the sample solutions were bubbled with pure Ar gas throughout the irradiation. The Ar-bubbling allows photoreduction only *via* electron transfer from $TiO_2$ as well as mixing of the heterogeneous solutions containing the photocatalysts

*Analysis and Characterization*

The composition (Si/Al ratio and Ti contents) of the synthesized zeolites were analyzed by using ICP-MS (Perkin-Elmer Elan 6000). The crystal state of the zeolites was characterized by XRD patterns measured by using a X-ray diffractometer (Mac Science Co. MO3X-HF model). In order to characterize the $TiO_2$ encapsulated into zeolites, IR spectra of the $TiO_2$-encapsulated zeolites were measured by using JASCO FT-IR-410 spectrophotometer. Absorption spectra of the $TiO_2$-encapsulated zeolites were also obtained by measuring diffuse reflectance with Shimadzu UV-3101PC spectro-photometer attached with integral sphere. In order to analyze the photoproduct of MO, the sample solutions were taken out

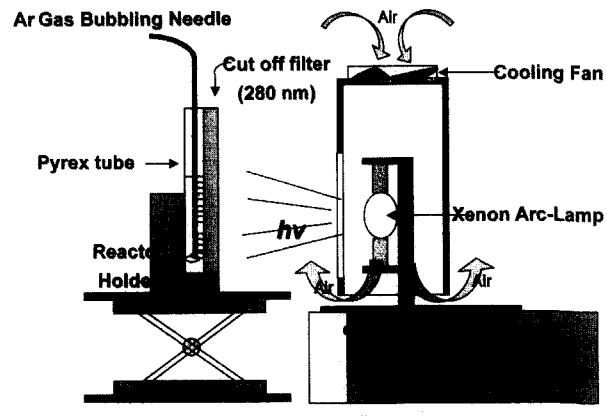


**Figure 1.** Scheme of photoreaction equipment.

at different time intervals during the photoreduction experiments. For the solutions containing photocatalysts, the solid powders were removed by filtering before analysis. The photodegradation product was identified by measuring absorption spectral changes of the MO solutions at different time during irradiation. The absorption spectra were measured by using SCINCO UV-VIS 2040 spectrophotometer.

## RESULTS AND DISCUSSION

*Characterization of $TiO_2$-entrapped zeolites*

Generally the removal of EFAL from normal zeolite is to remove the element Al existing on the surface of the zeolite framework by steaming treatments at lower temperature (below 100°C) or at higher temperature (above 200°C). Both steaming treatments do not change the Si/Al ratios (about 2.7-4.5) from those of normal zeolites, just replacing the tetrahedral aluminum of the framework with octahedral aluminum. Thus, these hot steaming treatments just change acidity and the stability of the framework, leading to form some amorphous zeolites. Therefore, in order to change the Si/Al ratio without side effects by the steaming treatments, it was necessary to treat the steamed zeolites with 2N nitric acid [19]. Table 1 shows the ICP-mass data for the prepared zeolites containing Si, Al and Ti. The Si/Al ratio of the $TiO_2$/EFAL-removed zeolites was determined to be 23, much higher than that of $TiO_2$/normal zeolites, indicating that the acid treatment of the hot steamed zeolite almost completely removes aluminum atoms on the framework.

In order to confirm the stablility and crystal state of the $TiO_2$/EFAL-removed zeolite Y, the X-ray diffraction patterns of all the prepared zeolites were measured as shown in Figure 2. Figure 2 (C) shows the XRD pattern of the $TiO_2$/EFAL-removed zeolite Y, which is the same as those of the normal zeolites (Figure 2 (A, B)), indicating that the crystal state is stable even after removal of the EFAL. However, the peak intensities in the 2θ range of 18-40 are weaker than those of the normal zeolites, even though the peaks below 18 attributed to the Si-framework structure show the same intensities as those of the normal zeolites. This must be due to the removal of Al from the framework without removal of Si. A quantity of Ti inside the zeolites was too small to be identified by XRD [23].

In order to identify Ti species inside the zeolites, FT-IR spectra of the $TiO_2$-encapsulated zeolites Y were measured as shown in Figure 3. The $TiO_2$/EFAL-removed zeolite Y shows different IR bands as compared with those observed from the

**Table 1.** ICP-Mass Analysis Data of Different Zeolites

| Zeolites | Al | Si | Ti | Si/Al |
|---|---|---|---|---|
| NaY-zeolite | 0.1159g | 0.2560g | - | 2.12 |
| $TiO_2$/normal zeolite Y | 0.0621g | 0.3058 | 0.0670g | 4.34 |
| $TiO_2$/EFAL removed zeolite Y | 0.0133g | 0.3060g | 0.0366g | 22.17 |

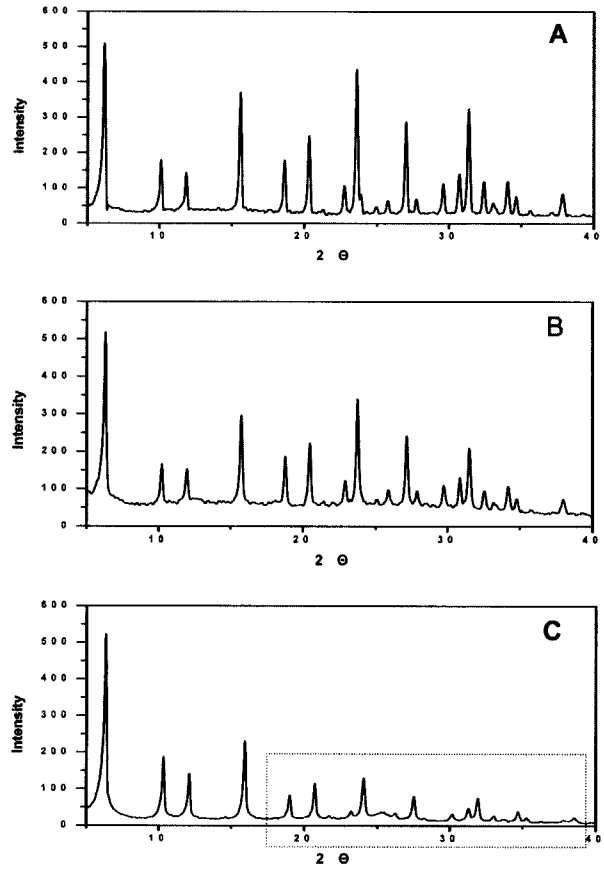


**Figure 2.** XRD Spectra of NaY zeolite(A), $TiO_2$/normal zeolite Y(B) and $TiO_2$/EFAL-removed zeoliteY(C).

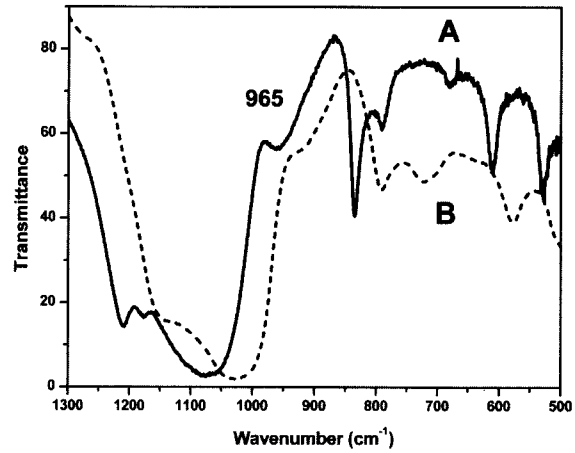


**Figure 3.** FT-IR spectra of $TiO_2$/EFAL removed zeolite Y(A) and $TiO_2$/normal zeolite Y(B).

$TiO_2$/normal zeolite Y, indicating that microenvironment of the $TiO_2$ in the EFAL-removed zeolite Y is different from that of normal zeolite Y. The 850 $cm^{-1}$ band corresponding to the Ti-O-Ti bond is clearly observed, indicating that Ti species exist in the form of $(TiO^{2+})_n$ clusters [23]. A band at 965 $cm^{-1}$ attributed to the Si-O-Ti bond [22] was also observed, indicating that the $(TiO^{2+})_n$ clusters are adsorbed on the

dealuminated Si-framework. These results are consistent with the data for the $TiO_2$-encapsulated zeolites Y reported before [20, 23], supporting the fact that $TiO_2$ is encapsulated inside the EFAL-removed zeolite Y. This is also confirmed by IR spectrum of pyridine adsorbed on $TiO_2$ /EFAL-removed zeolite. It shows the characteristic peaks at 1540 $cm^{-1}$, 1450 $cm^{-1}$ and 1490 $cm^{-1}$ (Figure 4), being attributed to the interaction of pyridine with Broenstead and Lewis acid site of the EFAL-removed zeolite [24].

Figure 5 shows the diffuse reflectance UV-VIS absorption spectrum of $TiO_2$/EFAL-removed zeolite Y. From this spectrum, the band gap energy of the encapsulated $TiO_2$ was determined to be 3.6 eV, which is higher than 3.2 eV of the anatase $TiO_2$. This implies that the size of $(TiO^{2+})_n$ cluster is much smaller than 10 nm of the anatase $TiO_2$.

*Photocatalytic reduction of MO*

The photoreduction of the sample azo dye, MO (5.0 x $10^{-5}$ M) was carried out in the presence of the 0.01g photocatalysts suspended in deaerated water. Figure 6 shows the absorption spectral changes of MO in the presence of $TiO_2$/normal zeolite Y (a) and $TiO_2$/EFAL-removed zeolite Y (b) in water upon illumination. The absorption intensities of MO at 465 nm were decreased with the appearance of a new absorption band at 250 nm. This indicates that MO is photodegraded to produce hydrazine derivatives through photoreduction by electrons ejected from the conduction band of $TiO_2$ in the zeolites. The concentrations (c) of hydrazine derivatives were calculated with the equation $A=\varepsilon$ cl by using molar extinction coefficient ($\varepsilon$=2.33 x$10^4$), where the path length (l) of the cell is 1 cm, and plotted as a function of irradiation time as shown in Figure 7. This plot shows that this photoreduction is pseudo first order with the rate constants of 2.07 x $10^{-7}$ mol $min^{-1}$ and

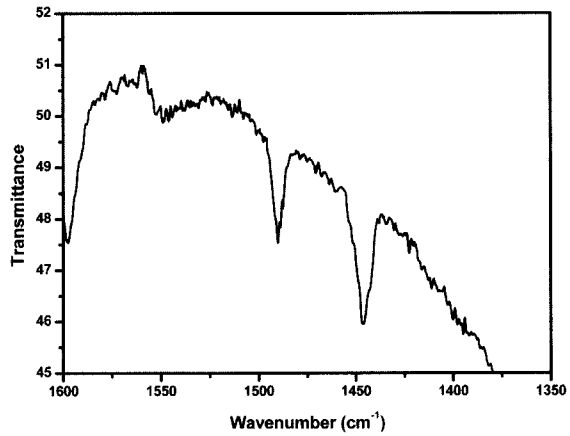


**Figure 4.** IR spectra of absorbed pyridine on the surface of $TiO_2$/ EFAL removed zeolite Y.

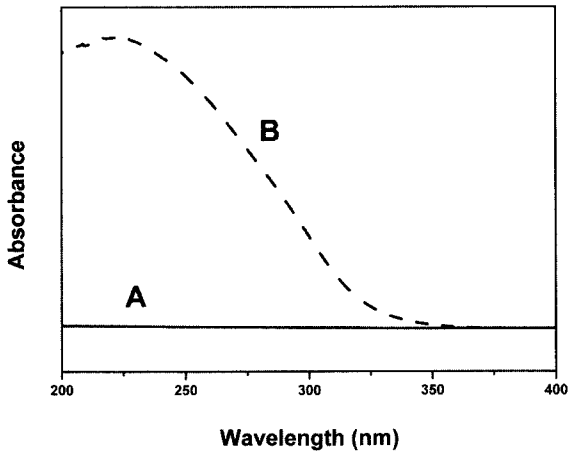


**Figure 5.** Diffuse reflectance UV-VIS spectra of HY zeolite(A), and $TiO_2$/EFAL removed zeolite Y(B).

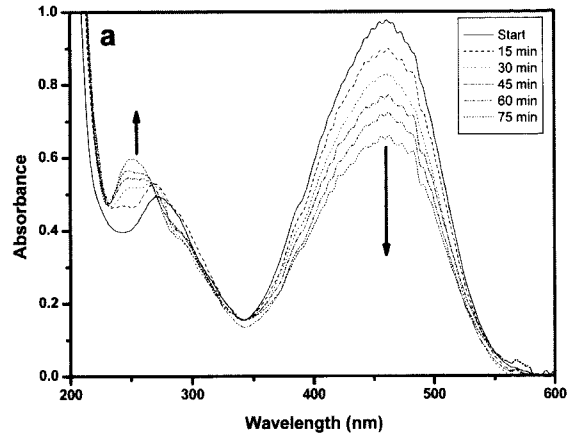


**Figure 6(a).** Absorption spectral change of methyl orange as a function of irradiation time (t) in the presence of $TiO_2$/normal zeolite Y. The initial concentration of methyl orange was is 5.0 × $10^{-5}$ M. The irradiation source is spectrally filtered with 280 nm long-pass filter.

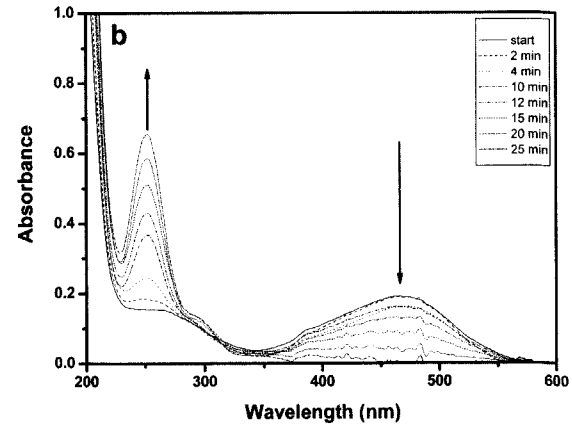


**Figure 6(b).** Absorption spectral change of methyl orange as a function of irradiation time(t) in the presence of $TiO_2$/EFAL removed zeolite Y. The initial concentration of methyl orange was is 5.0 × $10^{-5}$ M. The irradiation light is spectrally filtered with 280 nm long-pass filter.

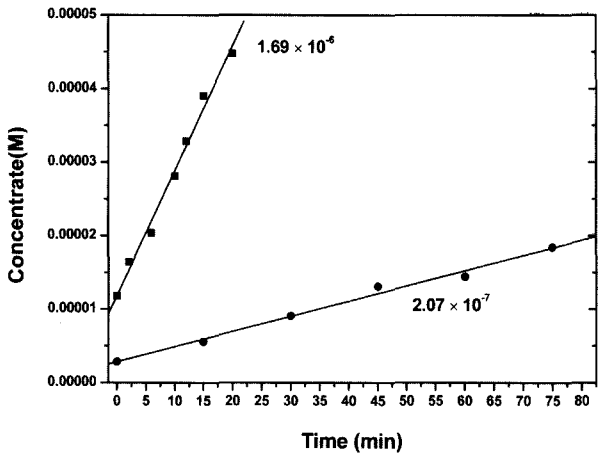


**Figure 7.** Plot of the absorption increase of hydrazine derivative at 250 nm as a function of irradiation time in the presence of $TiO_2$/normal zeolite Y(●) and $TiO_2$/EFAL-removed zeolite Y (■)

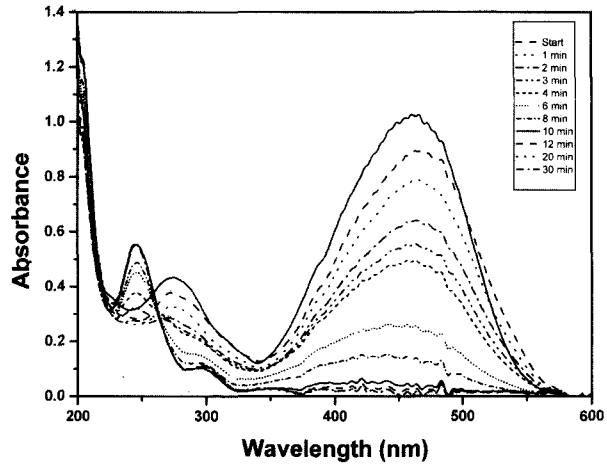


**Figure 8.** Absorption spectral change of methyl orange as a function of irradiation time(t) in the presence of Degussa P-25. The initial concentration of methyl orange is 5.0 × $10^{-5}$ M. The irradiation source is spectrally filtered with 280 nm long-pass filter.

1.69 x $10^{-6}$ mol $min^{-1}$ in the presence of $TiO_2$/normal zeolite Y and $TiO_2$/EFAL-removed zeolite Y, respectively. It is also noteworthy that the absorbance of MO at 465 nm measured in the presence of $TiO_2$/EFAL-removed zeolite Y before irradiation is much lower than that observed in the presence of $TiO_2$/normal zeolite Y, even though the initial concentration of MO was the same for both catalyst systems. This must be due to higher adsorption of MO in the $TiO_2$/EFAL-removed zeolite Y than in the $TiO_2$/normal zeolite Y. Supporting this, the red color was observed from the solid MO-containing $TiO_2$/EFAL-removed zeolite Y obtained by centrifuging the aqueous solution of MO mixed with $TiO_2$/EFAL-removed zeolite Y, whereas the filtrate solution shows orange color. On the other hand, the solid $TiO_2$/normal zeolite Y containing MO did not show noticeable color change. This indicates that MO-adsorbed site of the $TiO_2$/EFAL-removed zeolite Y is highly acidic (pH below 3.5) as compared to that of $TiO_2$/normal zeolite Y. Actually MO is a pH indicator near pKa = 3.5, and its orange color in the solution at pH higher than 3.5 is changed to red if pH of the solution is decreased to lower than 3.5. Thus, this observation leads us to suggest that MO is highly adsorbed on the highly acidic site of the framework of $TiO_2$/EFAL-removed zeolite Y (3.8 x $10^{-5}$ M MO adsorbed on 0.01 g of $TiO_2$/EFAL-removed zeolite Y). These results also suggest that the high adsorption of MO in the $TiO_2$/EFAL-removed zeolite Y enhances the photocatalytic efficiency for the reduction of the azo dye. This is consistent with the efficient production of of hydrazine derivatives (ca.95%), as shown in Figure 7, within 30 minutes after irradiation, implying that the adsorbed portion of MO is almost completely reduced. Further changes in absorption band of hydrazine at 250 nm were observed upon extended irradiation in the presence of $TiO_2$/EFAL-removed zeolite Y. The changes in absorption band of hydrazine derivatives were saturated from 30 minutes after irradiation. On the other hand, irradiation of MO in the presence of $TiO_2$/normal zeolite Y is still far from complete reduction after irradiation for 60 minutes.

The photocatalytic reduction of MO (5.0 x $10^{-5}$ M) in the presence of 1.0 g $TiO_2$/EFAL-removed zeolite Y was also compared with that in the presence of 1.0 g of Degussa P-25. Figure 8 shows the absorption spectral changes of MO upon irradiation in the presence of P-25. Initial absorbance of MO measured after filtration of Degussa P-25 was observed to a little lower than that of MO in the presence of $TiO_2$/EFAL-removed zeolite Y, implying that the adsorption of the azo dye is not so effective as $TiO_2$/EFAL-removed zeolite Y. Nevertheless, the photocatalytic degradation seems to be more efficient than that observed in the presence of $TiO_2$/normal zeolite Y, but it is less efficient that that observed in the presence of $TiO_2$/EFAL-removed zeolite Y. From the plot of the absorption changes at 250 nm as a function of irradiation time (Figure 9), the rate constants for the production of hydrazine derivatives were determined to be 10.4 x $10^{-2}$ $min^{-1}$ n the presence of $TiO_2$/EFAL-removed zeolite Y which is slightly higher than 8.6 x $10^{-2}$ $min^{-1}$ in the presence of Degussa P-25. However, it should be noticed that the amounts of the two catalysts (1.0 g) used are the same. In other words, the Degussa P-25 contains 1.0 g $TiO_2$,whereas 1.0 g of the $TiO_2$/EFAL-removed zeolite Y must contain much less than 1.0 g $TiO_2$, and the actual photocatalytic efficiency of the $TiO_2$/EFAL-removed zeolite Y should be much higher than P-25. This comparison again supports the fact that the efficient adsorption of MO in the zeolite framework contributes to enhance the photocatalytic efficiency of $TiO_2$/EFAL-removed zeolite Y. The framework of the $TiO_2$/EFAL-removed zeolite Y consists of Broenstead and Lewis acid sites so that azo group (-N=N-) can be hydrogen-bonded as shown in Scheme 1, enhancing the adsorption efficiency of azo-dye. Thus, the requirement of the substrate flux toward the reaction site is not necessary, and the

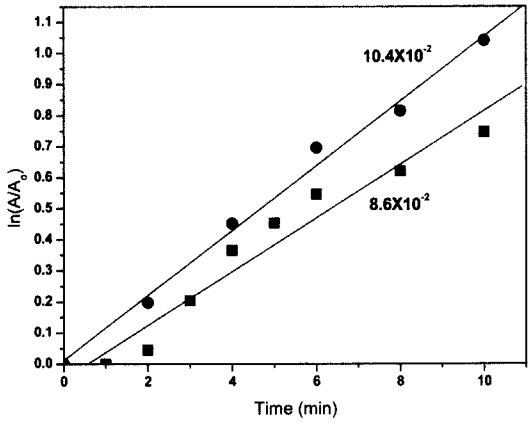


**Figure 9.** Plot of the absorption change of Hydrazine derivative at 250 nm as a function of irradiation time in the presence of $TiO_2$/EFAL removed zeolite Y (●) and P-25(■).

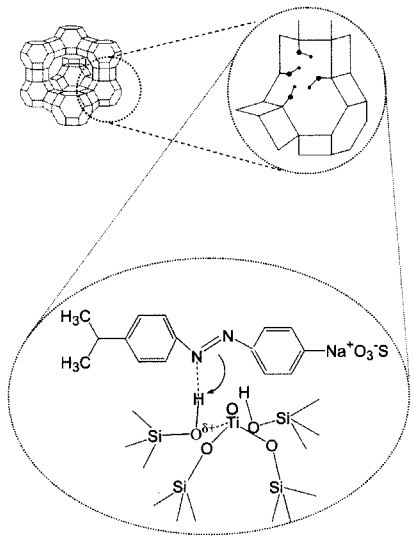


**Scheme 1.**

photocatalytic degradation can be done very efficiently with the $TiO_2$/EFAL-removed zeolite Y as compared with other photocatalysts.

Finally in order to check the possibility of repetitive use of the new photocatalyst, we have measured the photodegradation rates upon repetition of the photodegradation of MO by using the same photocatalyst. The $TiO_2$/EFAL-removed zeolite Y used once was irradiated for two more hours in order to completely photodegrade the residual MO adsorbed in the photocatalyst, and dried before using it again. Figure 10 shows the plot of the photodegradation of MO monitored by the production of hydrazine derivatives as a function of irradiation time upon repetitive use of the photocatalysts. This result demonstrates that the photodegradation rate of MO is decreased by about 10% upon each repetition of the use of the photocatalyst. Nevertheless, the new photocatalyst can be repetitively used at least about 5 times, keeping the effective

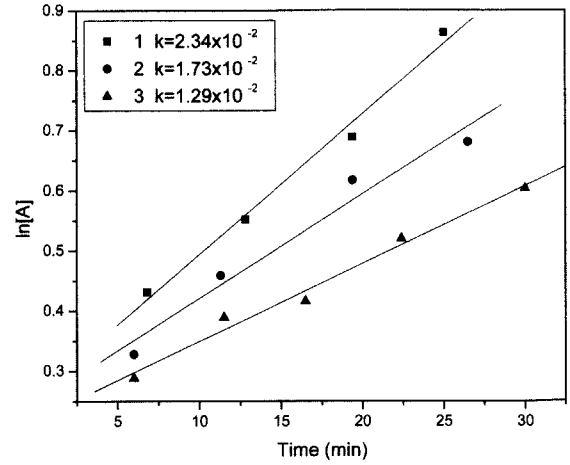


**Figure 10.** Plot of the absorption change of Hydrazine derivative at 250 nm as a function of irradiation time and repetition time in the presence of modified $TiO_2$/Y-zeolite.

photocatalytic activity. Thus, photodegradation of azo dyes can be done more effectively and economically by using the new photocatalyst, $TiO_2$/EFAL-removed zeolite Y rather than by using the commercially available Degussa P-25.

## ACKNOWLEDGEMENTS

This work has been financially supported by the Korea Science and Engineering Foundation (KOSEF) through the Center for Molecular Catalysis (CMC) at Seoul National University. W. J. Cho thanks the Chungnam National University Research Foundation for the research assistantship.

## REFERENCES

1. Spadaro, J. T., L. Isabelle, V. Renganathan (1994) Hydroxyl radical mediated degradation of azo dyes: evidence for benzene generation. *Environ. Sci. Technol.* **28**, 1389.
2. Nilsson, R., R. Nordlindre, U. Wass (1993) Asthma, rhinitis and dermatitis in workers exposed to reactive dyes. *British J. Ind. Medi.* **50**, 65.
3. Microbial Degradation of Xenobiotics and Recalcitrant Compounds Leisinger,T., A. M. Cook, J.R. Naesch (Eds.); Academic Press: London, UK, (1981).
4. Chung, K. T., G. E. Fulk, A.W. Andress (1981) Mutagenicity testing of some commonly used dyes. *Applied and Environmental Microbiology* **42**, 641.
5. Fujishima, A., K. Honda (1972) Electrochemical photolysis of water at a semiconductor electrode. *Nature* **238**, 37.
6. Rothenberger, G., J. Moser, M. Grätzel, N. Serpone, K. S. Devendra (1985) Charge carrier trapping and recombination dynamics in small semiconductor particles. *J. Am. Chem. Soc.* **107**, 8054.
7. Hidaka, H., Y. Asai, J. Zhao, K. Nohara, E. Pelizzetti, N. Serpone (1995) Photoelectrochemical decomposition of surfactants on a $TiO_2$/TCO particulate film electrode assembly. *J. Phys.*

*Chem.* **99**, 8244.
8. He, J., J. Zhao, T. Shen, H. Hidaka, N. Serpone (1997) Photosensitization of colloidal titania particles by electron injection from an excited organic dye-antennae function. *J. Phys. Chem. B* **101**, 9027.
9. Mills, A., S. Hunte (1997) An overview of semiconductor photocatalysis. *J. Photochem. Photobiol. A* **108**, 1.
10. Fox, M. A., M. T. Dulay (1993) Heterogeneous photocatalysis. *Chem. Rev.* **93**, 341.
11. Tang, W. Z., H. An (1995) UV/$TiO_2$ photocatalytic oxidation of commercial dyes in aqueous solution. *Chemosphere* **31**, 4157.
12. Zhu, C., L. Wang, L. Koug, X. Yang, L. Wang, S. Zheng, F. Chen, F. M. Zhi, H. Zong (2000) Photocatalytic degradation of Azo dyes by supported $TiO_2$ + UV in aqueous solution. *Chemosphere* **41**, 303.
13. Matthews, R. W. (1991) Photooxidative degradation of coloured organics in water using supported catalysts. $TiO_2$ on sand *Wat. Res.* **25**, 1169.
14. Sunada, F., A. Heller (1998) Effects of water, salt water and silicone overcoating of the $TiO_2$ photocatalyst of the rates and products of photocatalytic oxidation of liquid 3-octanol and 3-octanone. *Environ. Sci. Technol.* **32**, 282.
15. Takada, N., N. Iwata, T. Torimoto, H. Yoneyama (1998) Influence of carbon black as an adsorbent used in $TiO_2$ photocatalyst films on photodegradation behavior of propyzamide. *J. Catal.* **177**, 240.
16. Molecular Sieves , ACS Symposium Series 40, ed.; Katzer, J. R.; ACS: Washington DC (1977)
17. Zeolite Chemistry and Catalysis, ACS Monographs 171, ed.; Rado, J. A.; ACS: Washington DC (1976).
18. Zeolite Molecular Sieves; Breck, D. W.; Wiley: New York (1974).
19. Gola, A., B. Rebours, E. Milazzo, J. Lynch, E. Benazzi, S. Lacombe, L. Delevoye, C. Fernandez (2000) Effect of leaching agent in the dealumination of stabilized Y zeolites. *Microporous and Mesoporous Materials*. **40**, 73
20. Liu, X., K. Iu, K. J. Thomas, (1992) Encapsulation of $TiO_2$ in zeolite Y. *Chem. Phys. Lett.* **195**, 163.
21. Kim, Y., B. Lee, M. Yoon (1998) Excited-state intramolecular charge transfer of p-N,N-dimethylaminobenzoic acid in Y zeolites : hydrogen-bonding effects. *Chem. Phys. Lett.* **286**, 466.
22. Duprey, E., P. Beaunier, M.-A. Springnel-Huet, F. Bozon-Verduraz, J. Fraissaed, J.-M. Manoli, J.-M. Bregeault (1997) Characterization of catalysts based on titanium silicalite, TS-1, by physicochemical techniques. *J. Catalysis* **165**, 22.
23. Kim, Y., M. Yoon (2001) $TiO_2$/Y-zeolite encapsulating intramolecular charge transfer molecules : a new photocatalyst for photoreduction of methyl orange in aqueous medium. *J. Mol. Catal. A: Chem.* **168**, 257.
24. Corma, A., V. Fornes, M. T. Navarro, J. Perez-Pariente (1994) Acidity and stability of MCM-41 crystalline aluminosilicates. *J. Catalysis* **148**, 569.